

# High Resolution X-ray spectroscopy of Cataclysmic Variables

K.P. Singh

Tata Institute of Fundamental  
Research, Mumbai

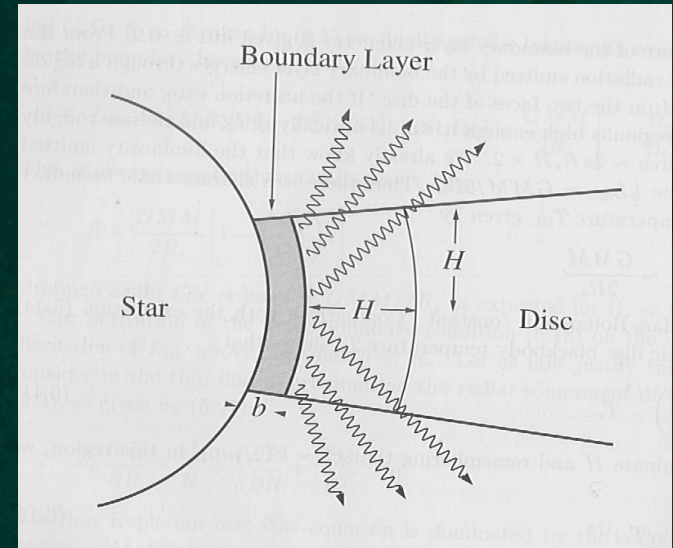
Wideband X-ray Astronomy:  
Frontiers at IUCAA, Jan 13, 2010

# Non-magnetic CVs: Dwarf Novae

1. Accretion Disk (5000 K – few  $\times 10^4$  K) Optical to far UV. Half of the gravitational potential energy of the accreting material is released.

2. Boundary layer (between WD and inner edge of the disk)

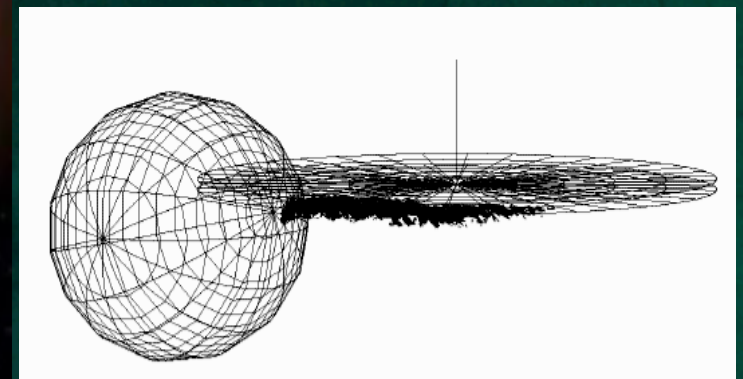
High accretion rate  $\sim 10^{-8} M_{\odot}/\text{yr}$  – EUV, soft X-ray  
Low accretion rate  $\sim 10^{-11} M_{\odot}/\text{yr}$  – hard X-ray



Secondary Star

White Dwarf

Accretion Disk



Accretion stream

# Magnetic CVs

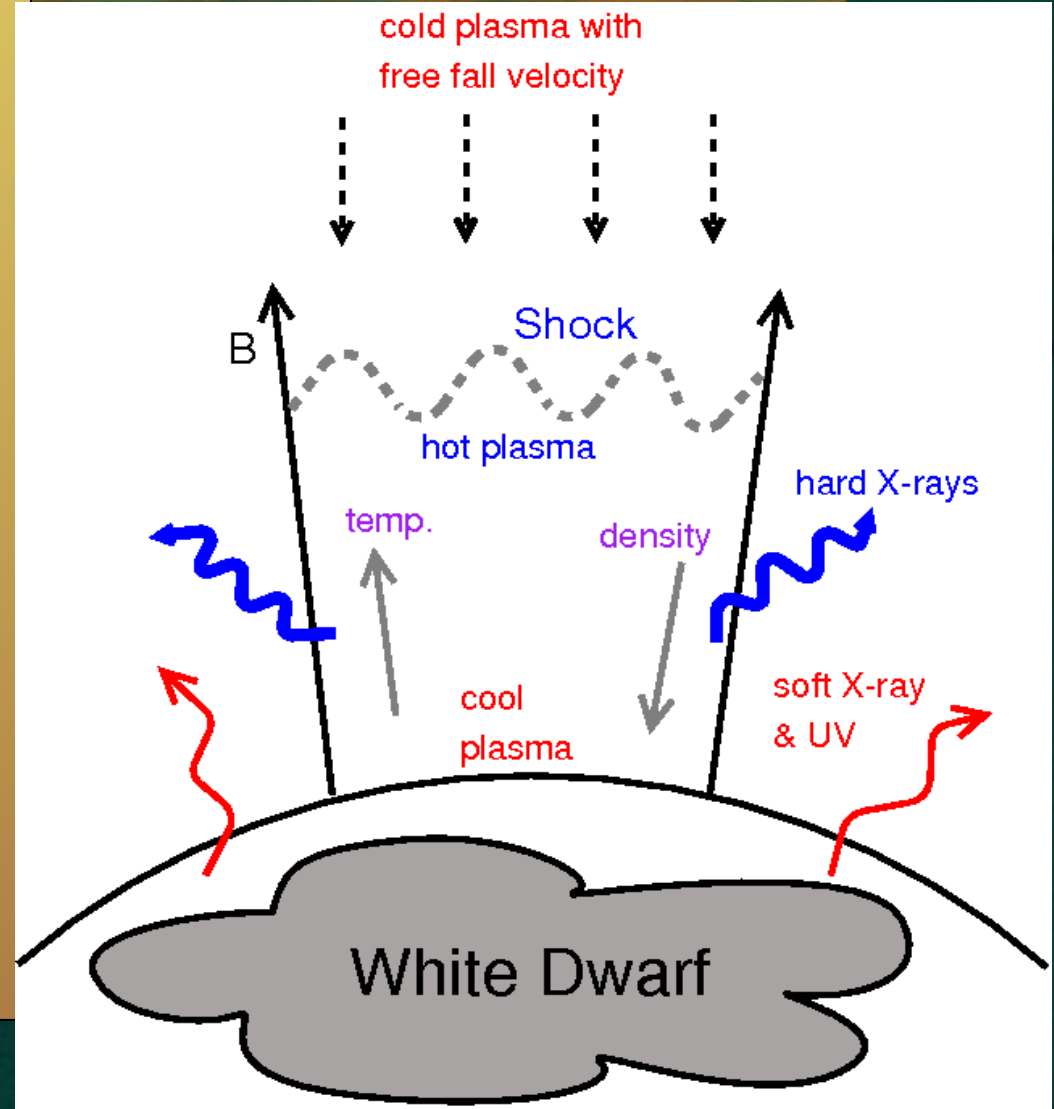
Intermediate Polars  
(IPs)

Polars

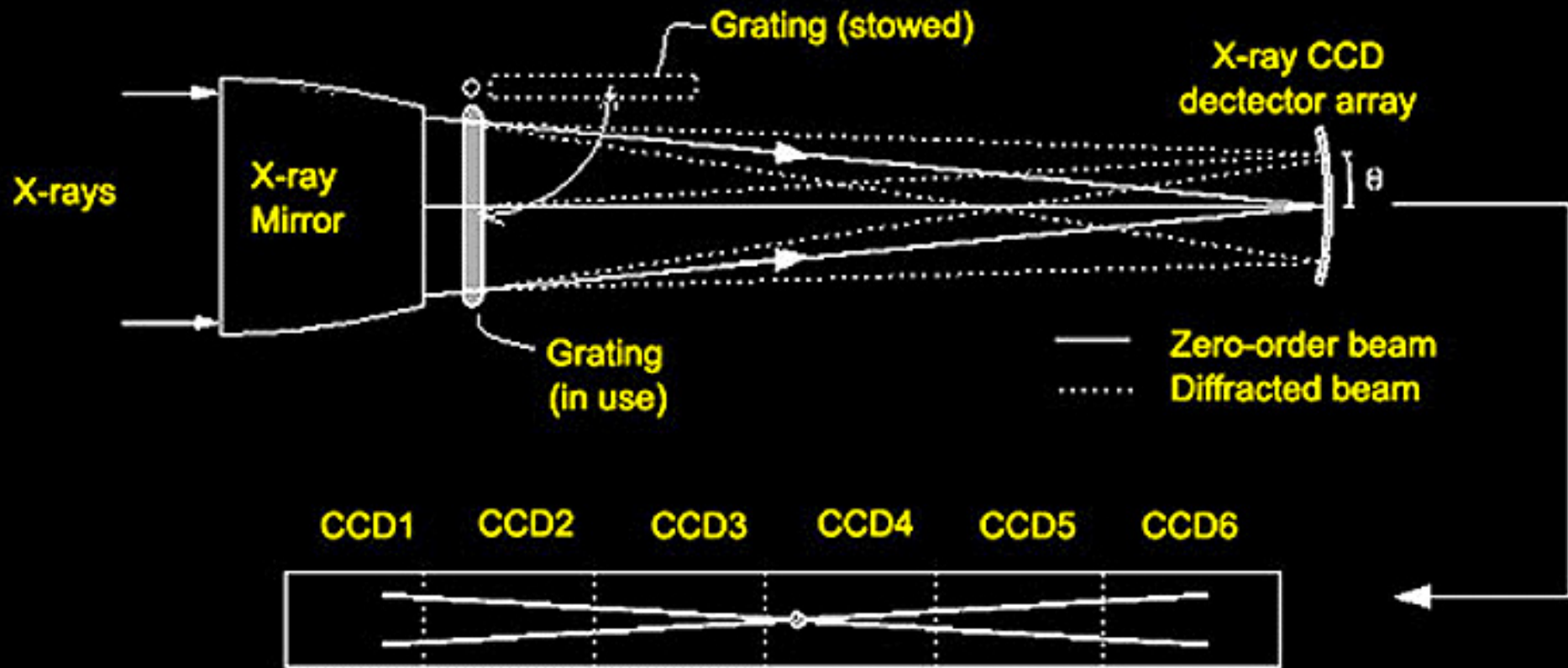


# Magnetic CVs

- Accreting material follows magnetic field lines and directly falls onto the white dwarf.
- Forms a strong shock near the surface of the white dwarf.
- Continuous temperature distribution
- Temperature and density gradient
- Line emission from post-shock plasma



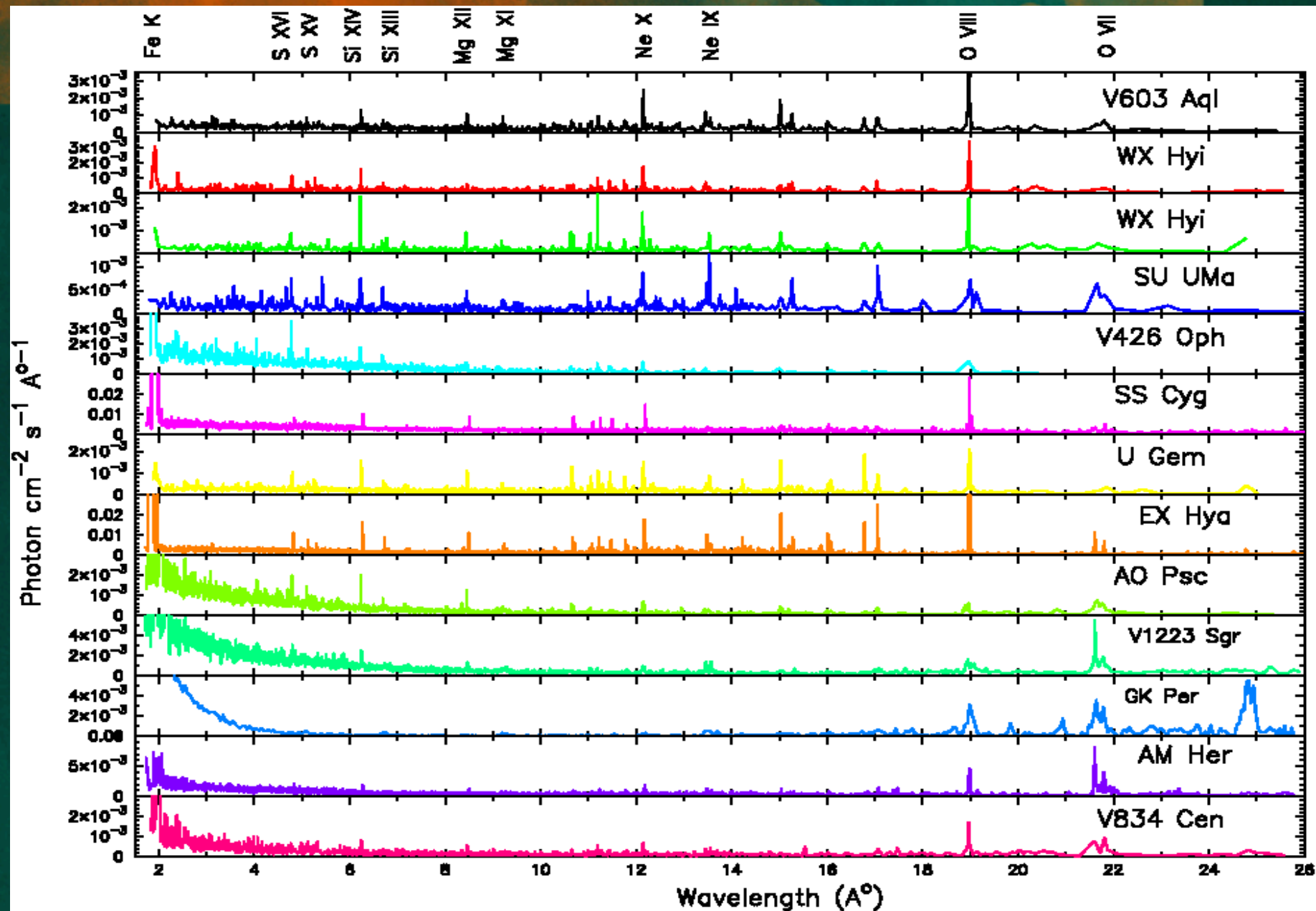
# Chandra Gratings: HETG, LETG



HETG: Energy band 0.4-10 keV.

Resolving power ( $E/\Delta E$ ) varies from  $\sim 800$  at 1.5 keV to  $\sim 200$  at 6 keV

# MEG spectra of 12 CVs in quiescence



# Analyzing high resolution X-ray spectra

## 1) Global fit approach:

- To find a plasma model that better represent the observed spectrum in terms of emission lines
- To estimate the temperature distribution in the emitting regions

## 2) Line-by-line fit approach:

- Using several Gaussians representing emission lines
- To study the line profile in detail and obtain line parameters like position, width and flux
- Using line ratios to study the temperature, density, ionization stage, emission geometry, opacity in the emitting plasma
- To understand the dominant physical process in plasma and accretion physics.

# Fe $K\alpha$ Line Study of non-Magnetic CVs

## Chandra $\pm 1$ order HEG spectra for 6 CVs

**Fe  $K\alpha$  Lines:** Fluorescent line @ 6.4 keV  $\rightarrow$  1 Gaussian  
He-like triplets @ 6.7002 (r), 6.6821 ( $i_1$ ), 6.6673 ( $i_2$ )  
and 6.6364 keV  $\rightarrow$  3 Gaussians  
H-like doublets @ 6.973 and 6.952 keV  $\rightarrow$  1 Gaussian

**H and He-like lines and their ratio**  $\rightarrow$  Regions of highest temperature in the boundary layer of non-MCVs and the ionization temp.

**G-ratio =  $(f+i)/r$**   $\rightarrow$  sensitive to electron temperature

**R-ratio =  $f/i$**   $\rightarrow$  sensitive to electron density

**Fluorescent line**  $\rightarrow$  cold material and reflection

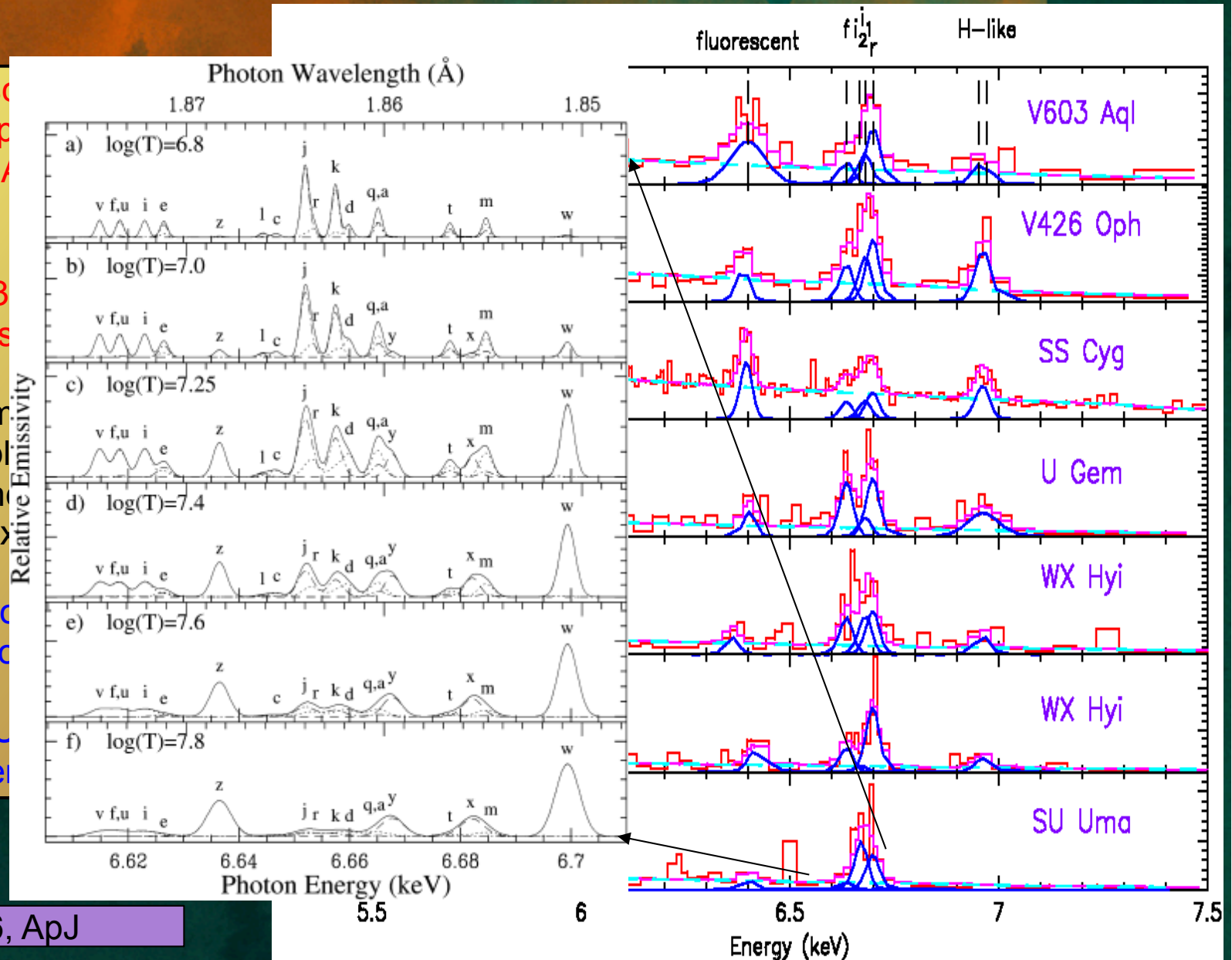
# Fe K $\alpha$ Lines in Quiescence

Prominent fluorescent Fe K $\alpha$  lines in V603 Aql, V426 Oph  
 $\Rightarrow$  reflection from the inner disk surface as seen in the presence of weak absorption.

It is broad in V603 Aql, corresponding to a velocity of  $1700 \pm 1000$  km/s.

Stronger r-line components are seen in He-like triplets in U Gem, indicating the dominance of primary Fe K $\alpha$  lines in the DES with  $T > 3 \times 10^7$  K.

U Gem showed broad Fe K $\alpha$  lines that corresponds to a velocity of  $1400 \pm 800$  km/s. It is absent in SU UMa. The plasma is at low temperature.



# Fe $K\alpha$ Lines in Outburst

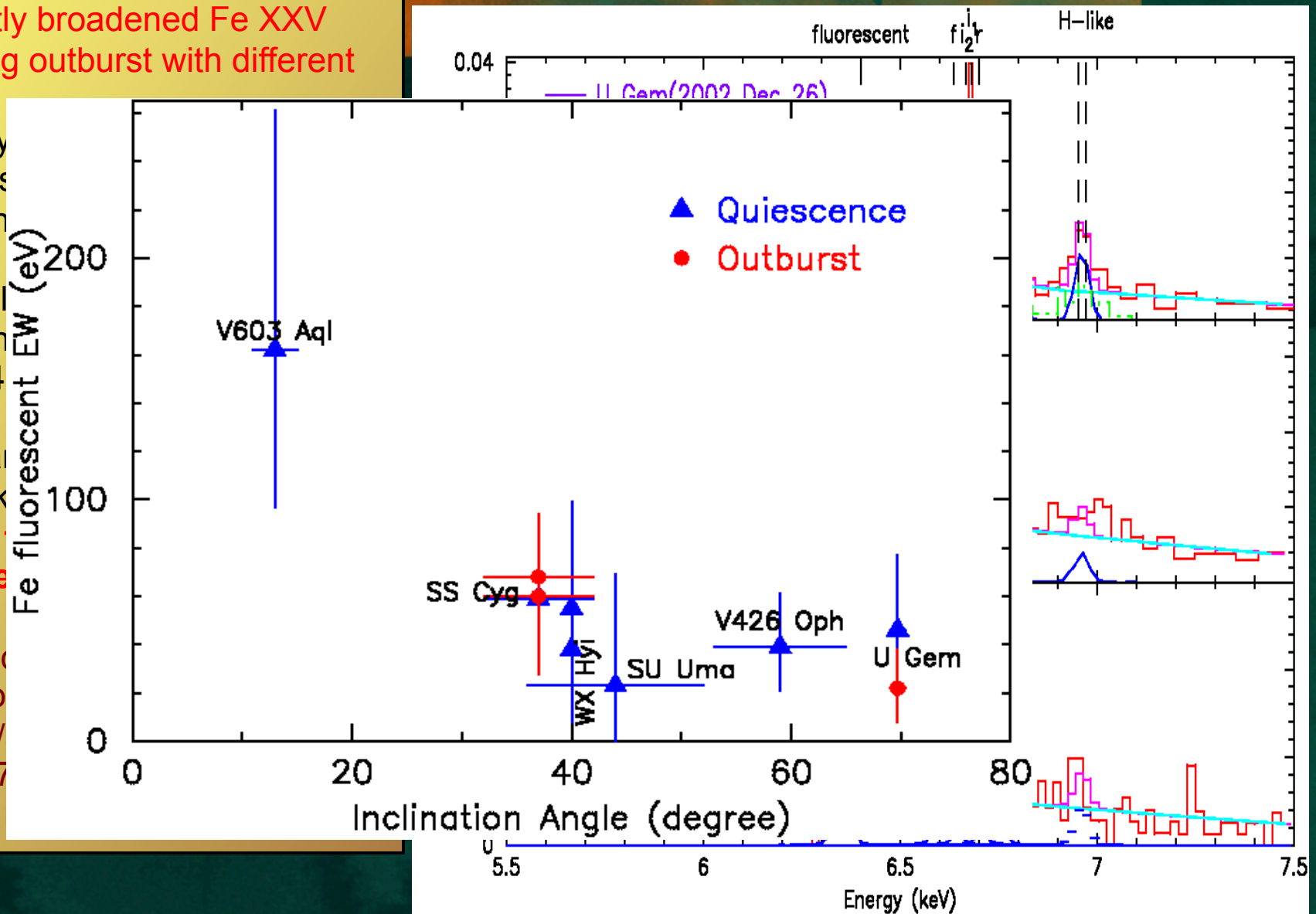
Significantly broadened Fe XXV lines during outburst with different profiles.

U Gem: Sy  
Gaussian s  
each line h  
km/s.

SS Cyg: Fl  
shifted r lin  
( $1120 \pm 224$   
and f lines  
O-type star  
galaxy Mrk

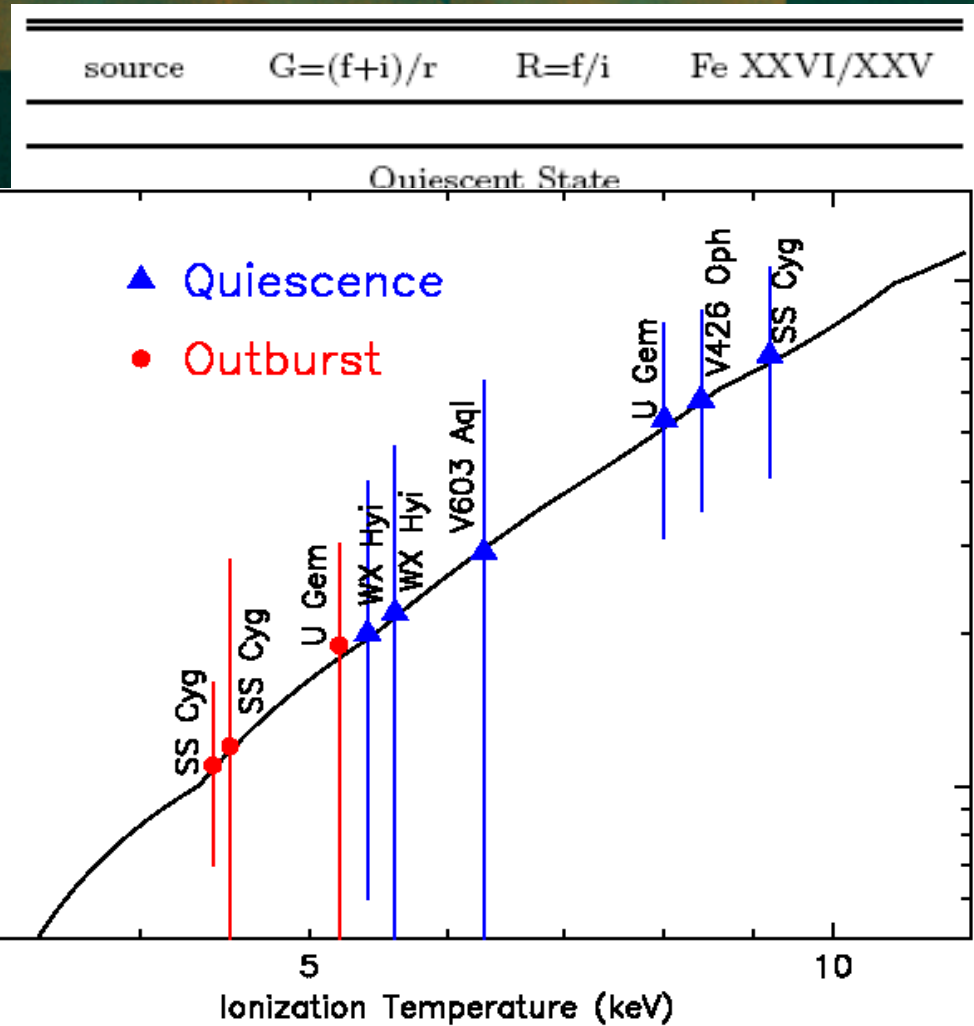
**Evidence  
during the**

Red-shifted  
SS Cyg co  
 $\sim 2300$  km/  
GK Per: 37  
pre-shock



# Plasma diagnostics: G and R ratios

- Principal lines can be used to estimate the G & R ratios.
- G-ratio is close to 1 for most of the sources  $\Rightarrow$  the plasma is in CIE.
- SS Cyg has  $G \sim 2.4 \Rightarrow$  hybrid
- SS Cyg, V603 Aql, V426 Oph and WX Hyi the R-ratio varies in 0-2.5, hence not constrain the plasma density.
- Better signal-to-noise data are rare



Fe XXVI/Fe XXV line flux ratio provides Ionization temperature.  
 $kT_{ion} \leq 12$  keV for all non-magnetic CVs studied.  
 For SS Cyg the  $kT_{ion}$  is higher during quiescence than outburst.

# G ratio for other elements (O, Mg, S and Si) for 12 CVs

Solid curves: coronal plasma

Dashed curves: including satellite lines and under photo-ionization conditions

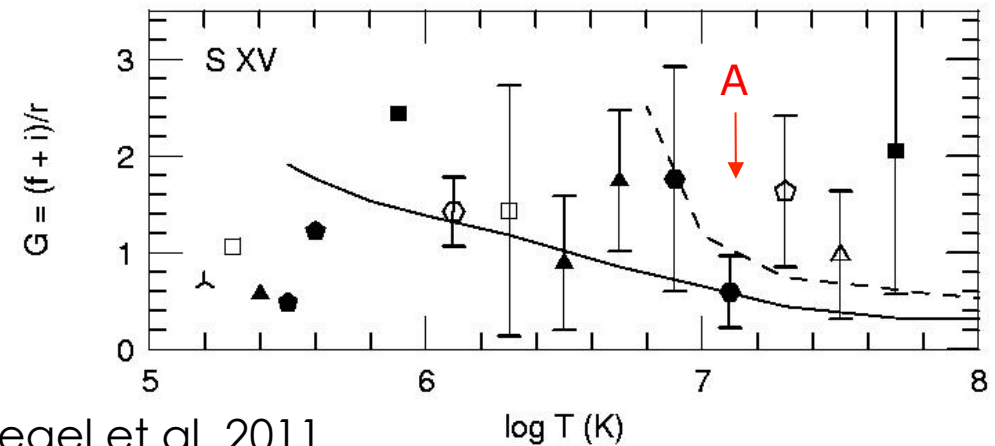
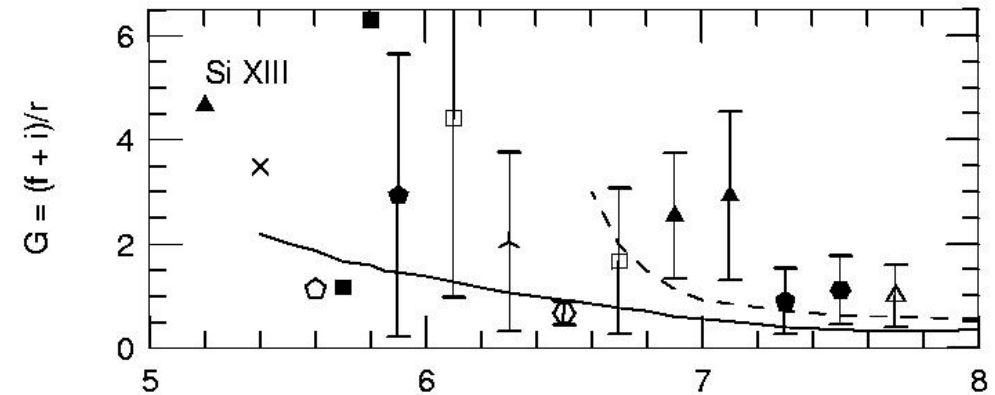
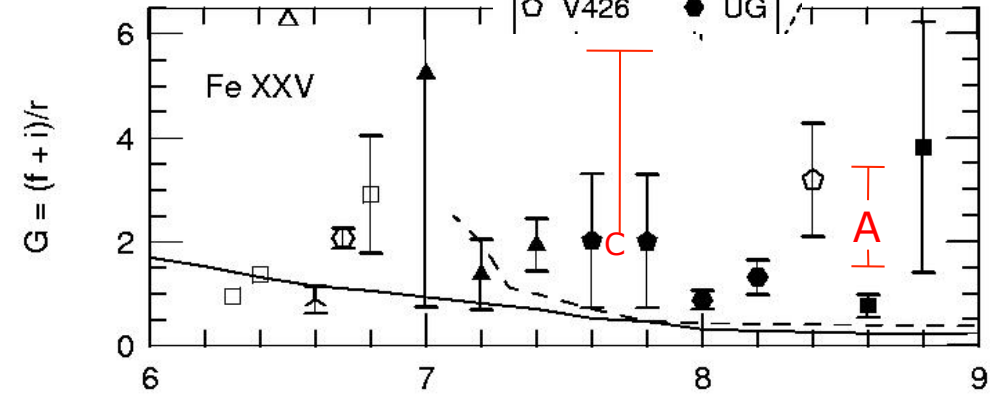
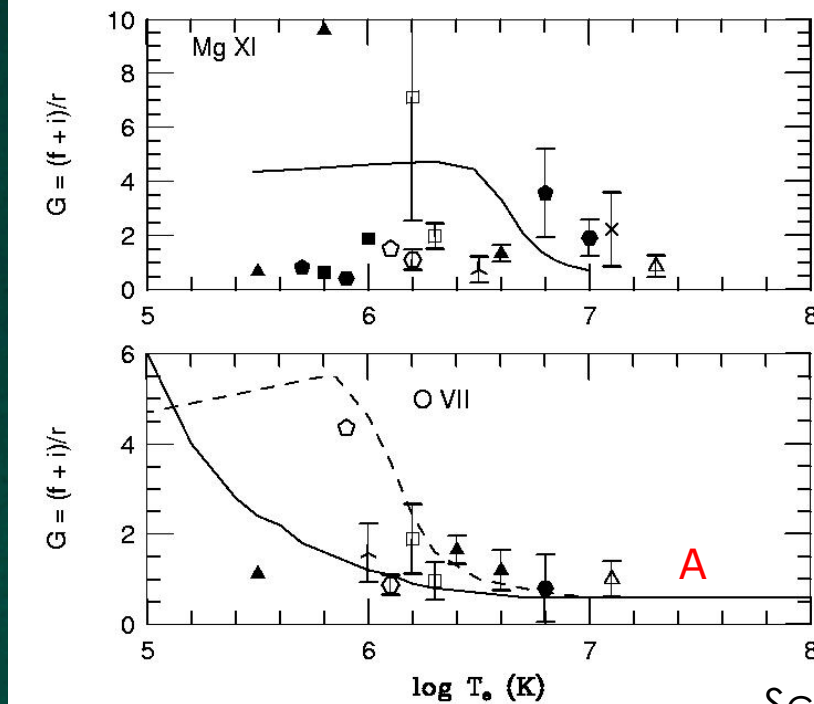
Bautista & Kallman (2000) Fe, Si, S, O

Porquet & Dubau (2000) Mg

Collisional ionization with low T or photoionization with high T ?

Key	
x	V1223
∧	AO
△	V603
□	GK
○	V426
○	EX
▲	SS
■	WX
●	SU
●	UG

A: AM Her  
C: V834 Cen



# R ratio: Plasma Density

## Log Ne for

Fe: > 15-16 cm<sup>-3</sup>

S : > 14 cm<sup>-3</sup>

Si: > 11.5 cm<sup>-3</sup>

Mg: > 12 cm<sup>-3</sup>

O: > 10 cm<sup>-3</sup>

Absence of Fe XXI

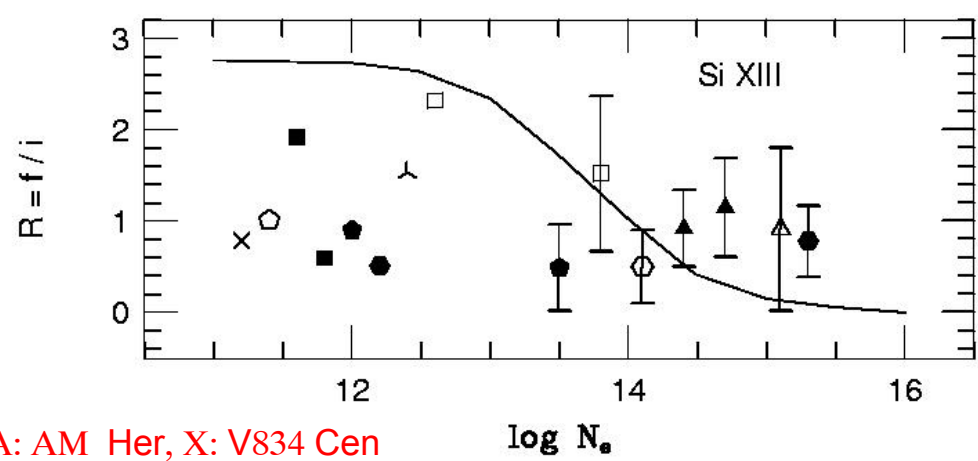
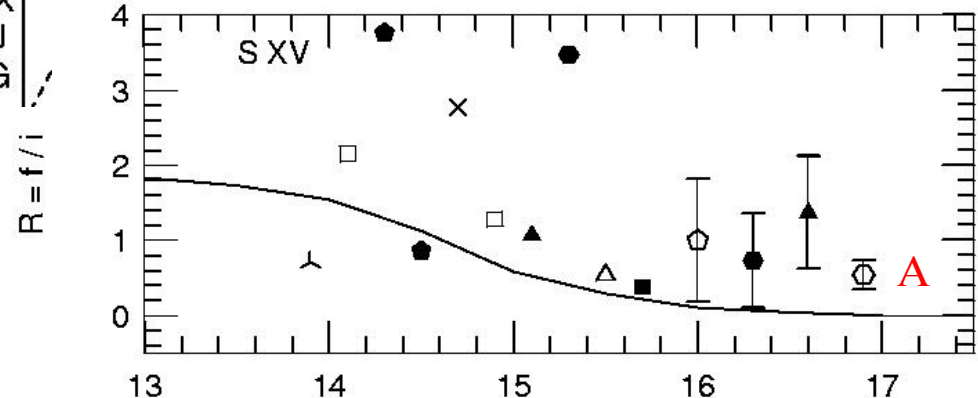
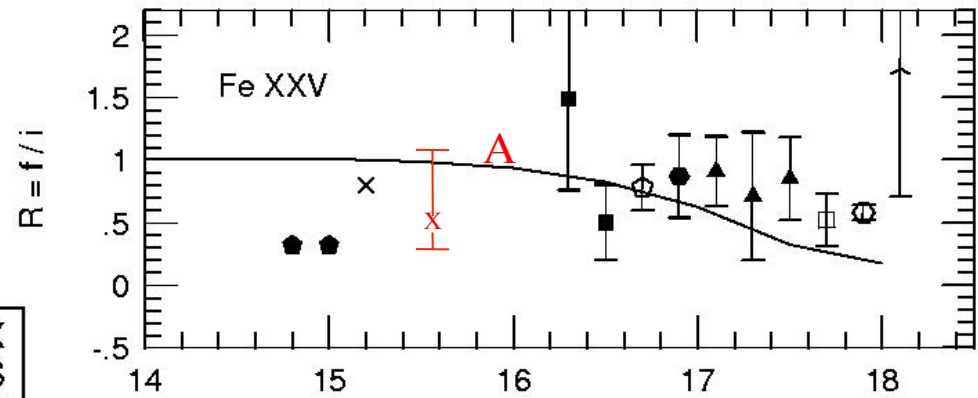
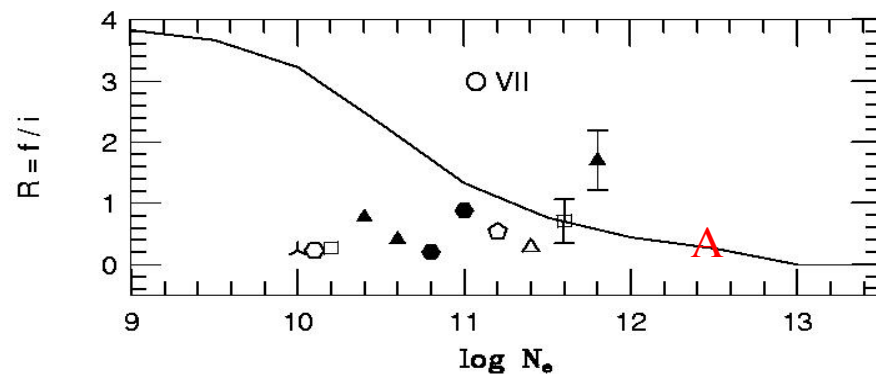
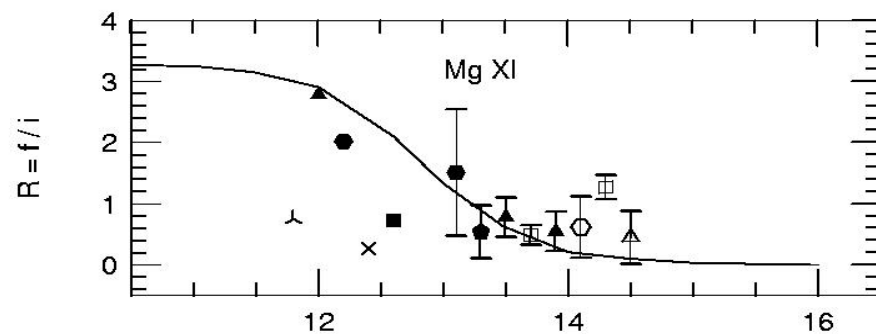
12.26 A gives log

Ne > 13

## Ratios Immune from UV:

Fe XVII 17.10 to 17.05 &  
17.10 to 16.77 Log Ne > 14

Key			
×	V1223	○	EX
∧	AO	▲	SS
△	V603	■	WX
□	GK	●	SU
○	V426	●	UG



A: AM Her, X: V834 Cen

log N<sub>e</sub>

# Ne/O Abundance (12 CVs)

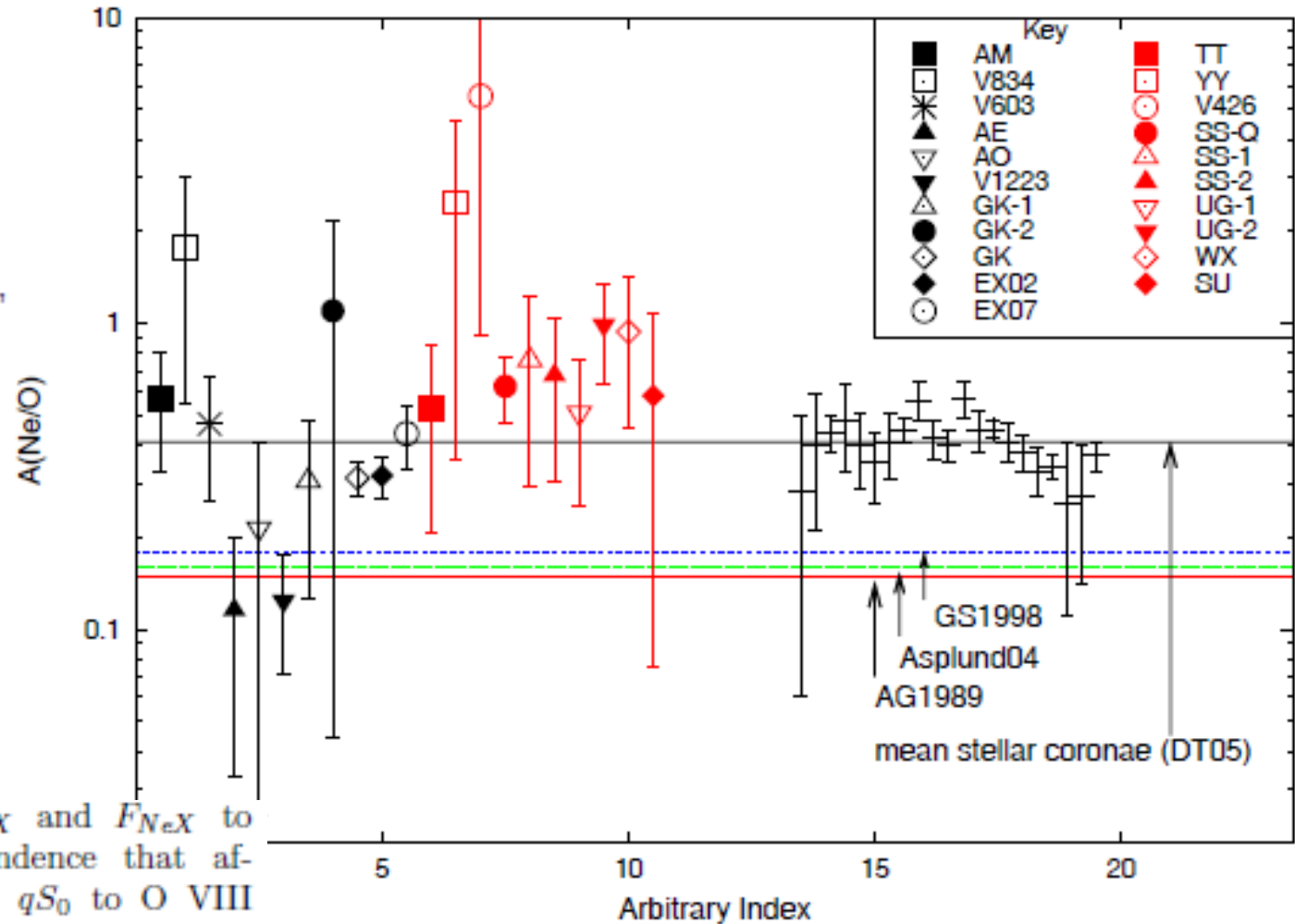
$$\frac{A_{Ne}}{A_O} = \left(\frac{G_O}{G_{Ne}}\right) \frac{F_{Ne}}{F_O}$$

$$F_{ji} = \int_{\Delta T_{ji}} G_{ji}(T) \Phi(T) dT$$

Adopting Drake & Testa(2005) prescription used for Nearby stars.

algebraic combination of  $F_{NeIX}$  and  $F_{NeX}$  to remove the temperature dependence that affects the Ne IX  $1s2p^1 P_1 \rightarrow 1s^2 qS_0$  to O VIII  $2p^2 P_{3/2,1/2} \rightarrow 1s^2 S_{1/2}$  ratio. The corrected flux ratio that results is

$$\frac{F_{NeIX} + 0.15F_{NeX}}{F_O}$$

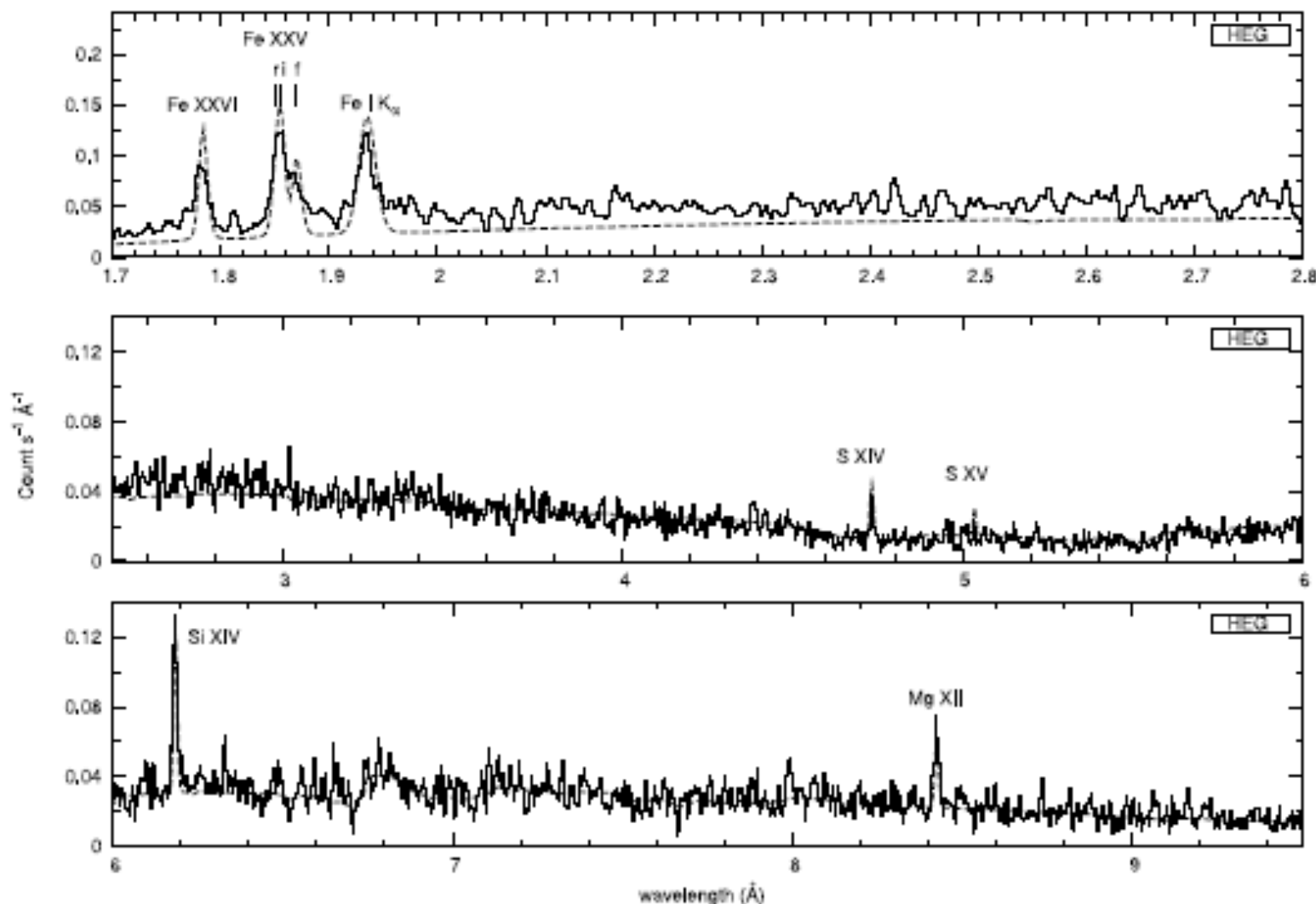


Mean = 0.44±0.32 IPs and 0.72±0.18 DNe  
 ONe models of WDs preferred over CO  
 models of Jose & Hernandez (Schlegel et al. 2011)

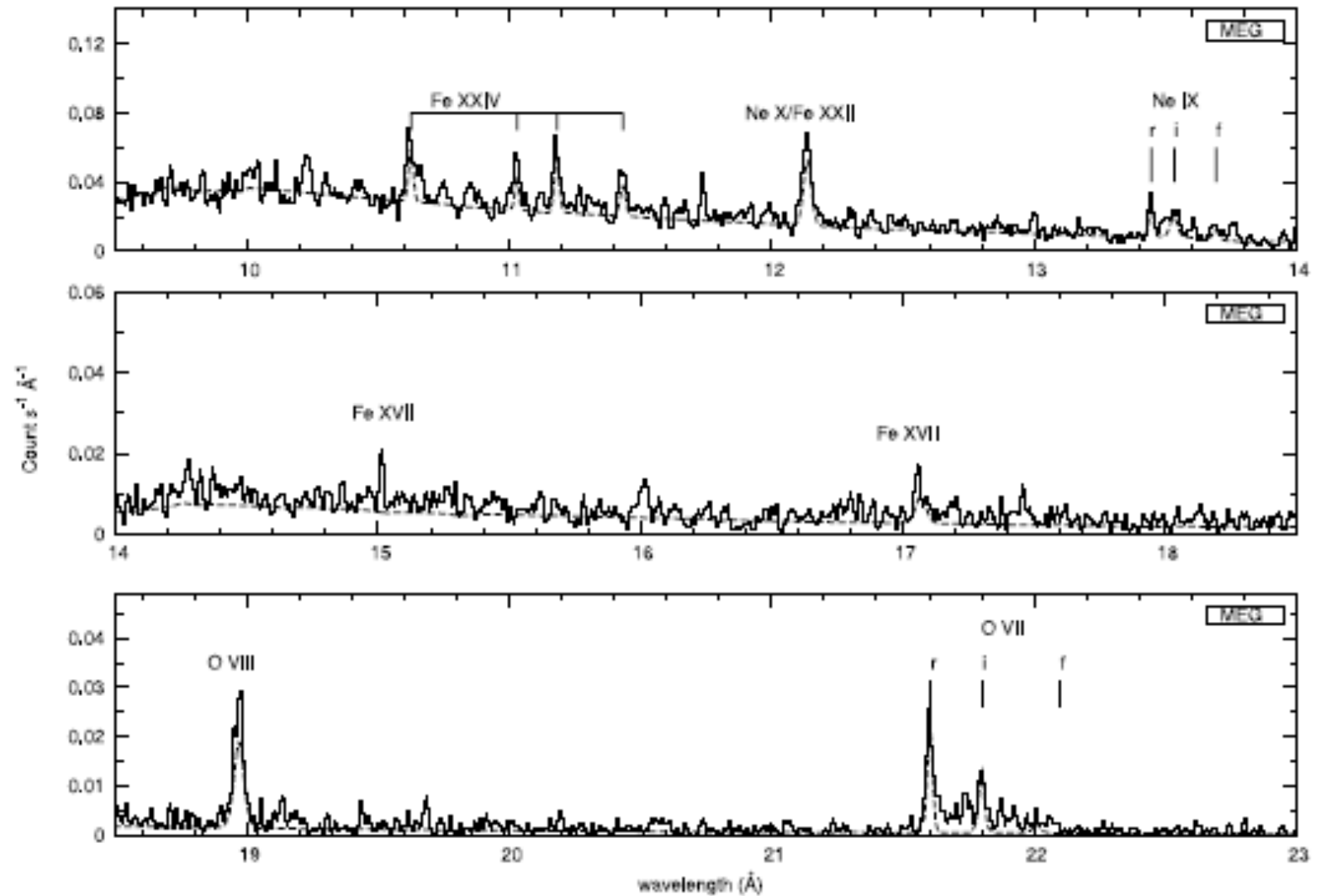
# Chandra HETG Spectrum of AM Her

- Strong fluorescent line of Fe  $K\alpha$  is seen
- Relative strength of r with respect to i indicates the importance of collisional processes
- Flux ratio  $R = f/i$  for Ne IX & O VII predicts a density  $n_e = 4 \times 10^{12} \text{ cm}^{-3}$ .
- The ratio  $G = (f + i)/r$  for the two ions gives T of 2 MK.

GIRISH, RANA, & SINGH



# Chandra MEG Spectrum of AM Her



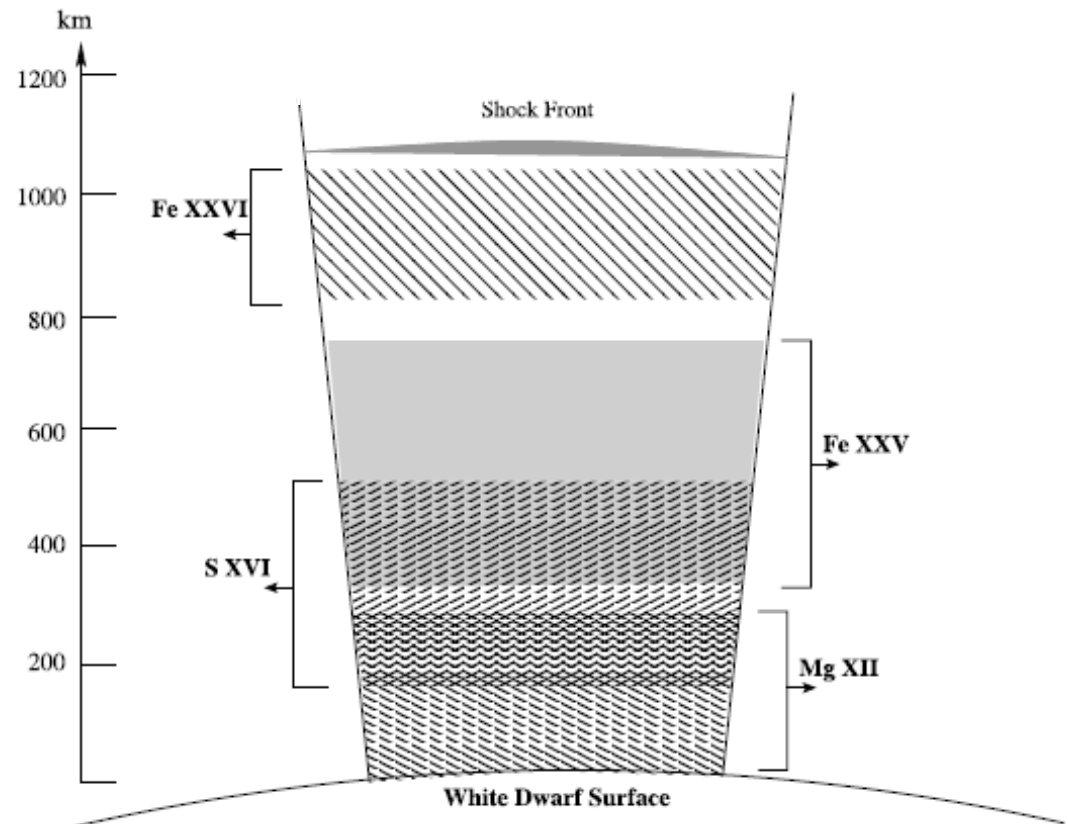
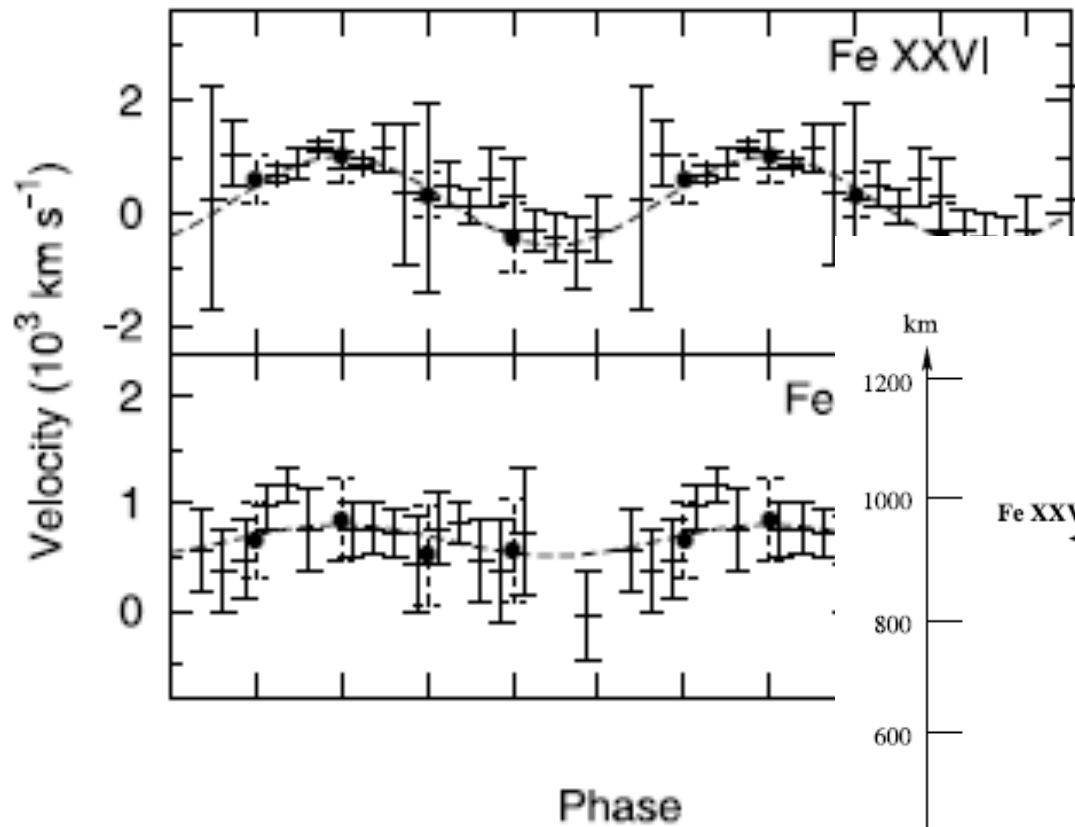


# Phase Resolved Spectroscopy of AM Her

## Her

• Line centers of Mg XII, Si XVI, resonance line of Fe XXV, and Fe XXVI emission modulated by 1000 km/s indicating bulk motion of ionised material in the accretion column. Using Aizu

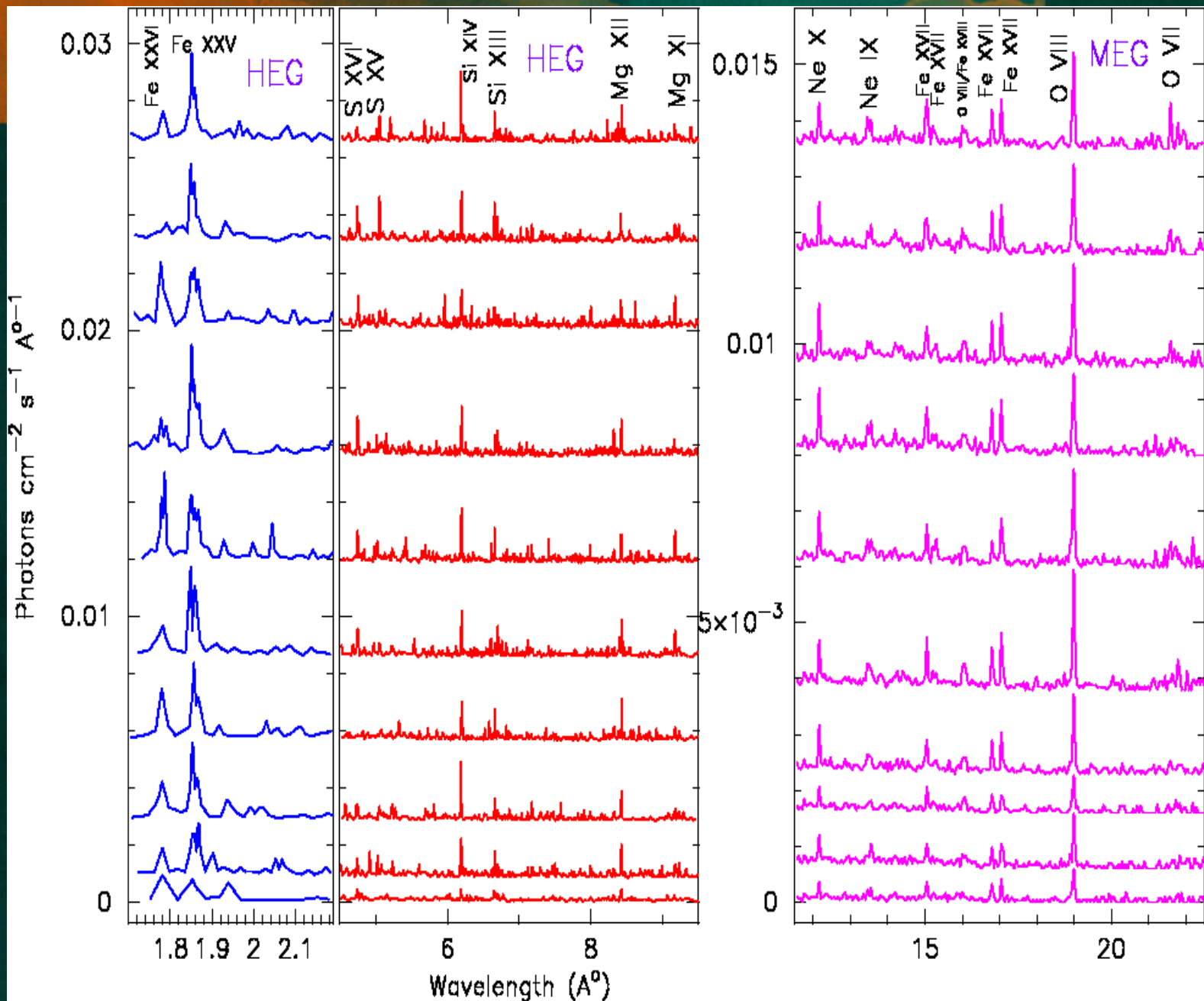
GIRISH, RANA, & SINGH



# EX Hya: Binary phase resolved spectra (60 ks)

H-like lines  
dominate  
from O to  
Si

He-like lines  
dominate  
for Fe  
except  
during the  
phases  
centered  
on 0.3 and  
0.5



# EX Hydrae: Spin Phase folding Fe and S lines (500 ks)

Fig. 35.— Light curve for EX Hya folded at the spin phase: (left) Fe XXVI  $K\alpha$  and Fe XXV r; (right) Fe XXV i and f. In this and all subsequent light curves, the filled squares represent the light curve of the neighboring continuum.

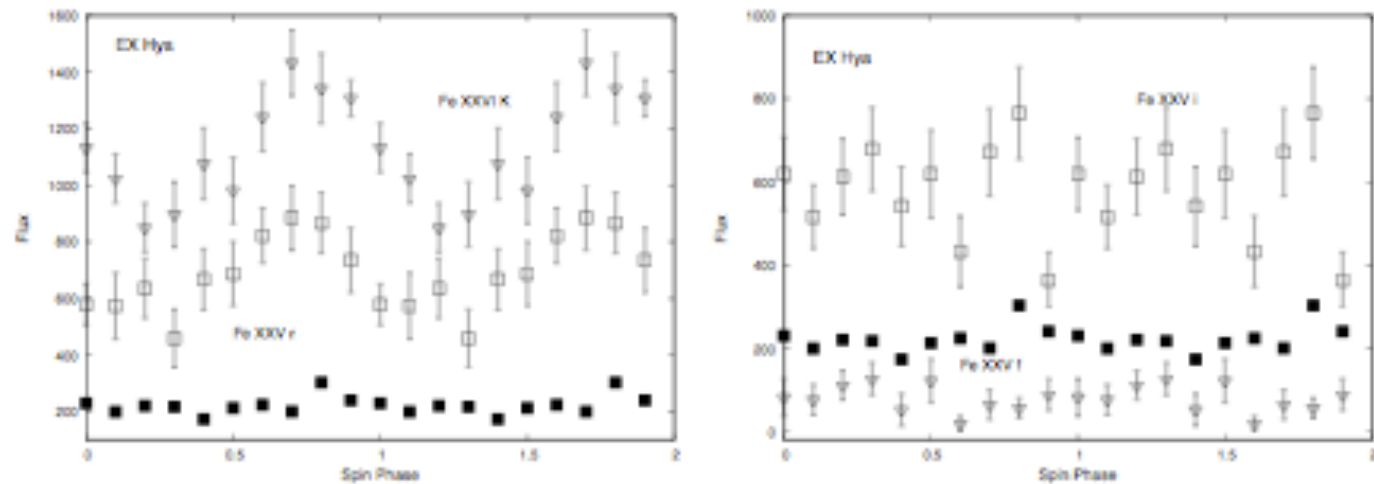
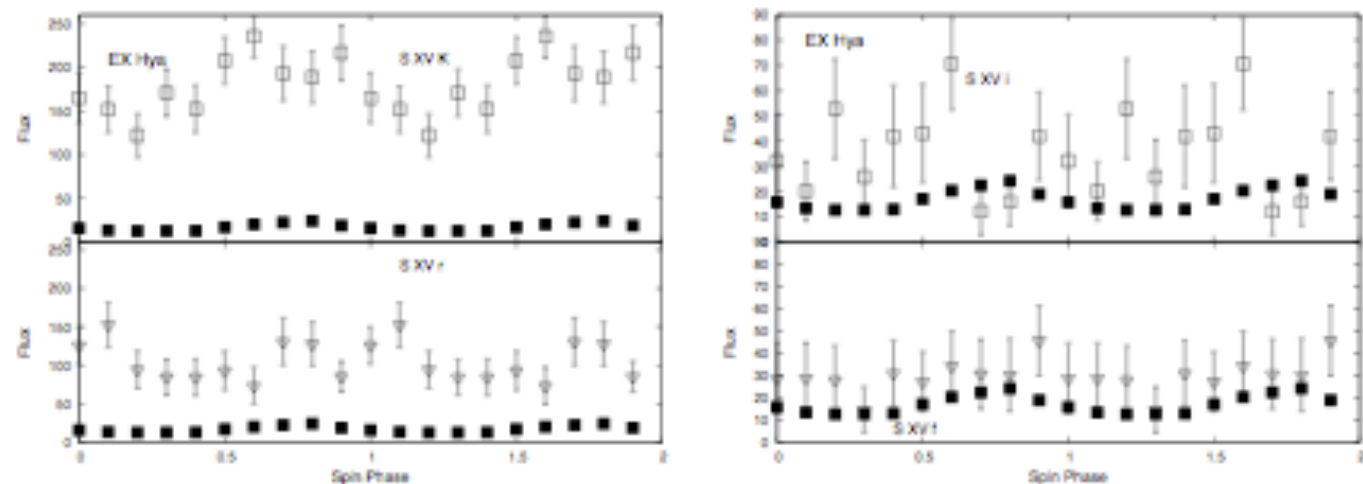


Fig. 36.— Light curve for EX Hya folded at the spin phase: (left) S XVI  $K\alpha$  and S XXV r; (right) S XV i and f. Filled squares = neighboring continuum.



# EX Hydrae: Spin Phase folding Si and Mg lines

Fig. 37.— Light curve for EX Hya folded at the spin phase: (left) Si XIV  $K\alpha$  and Si XIII r; (right) Si XIII i and f. Filled squares = neighboring continuum.

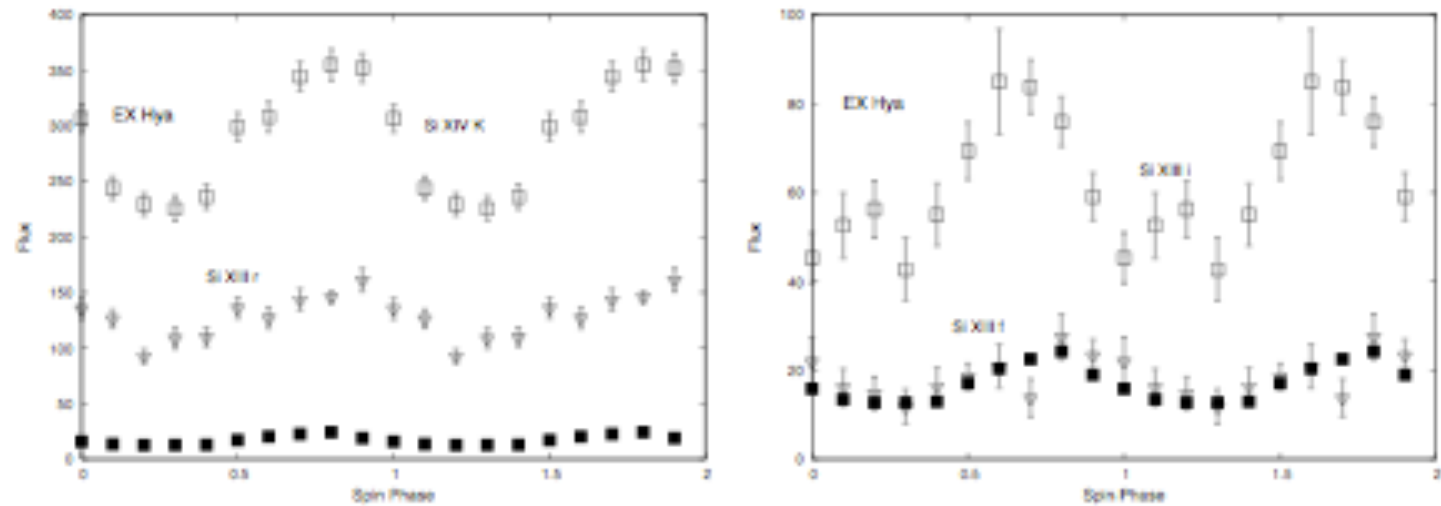
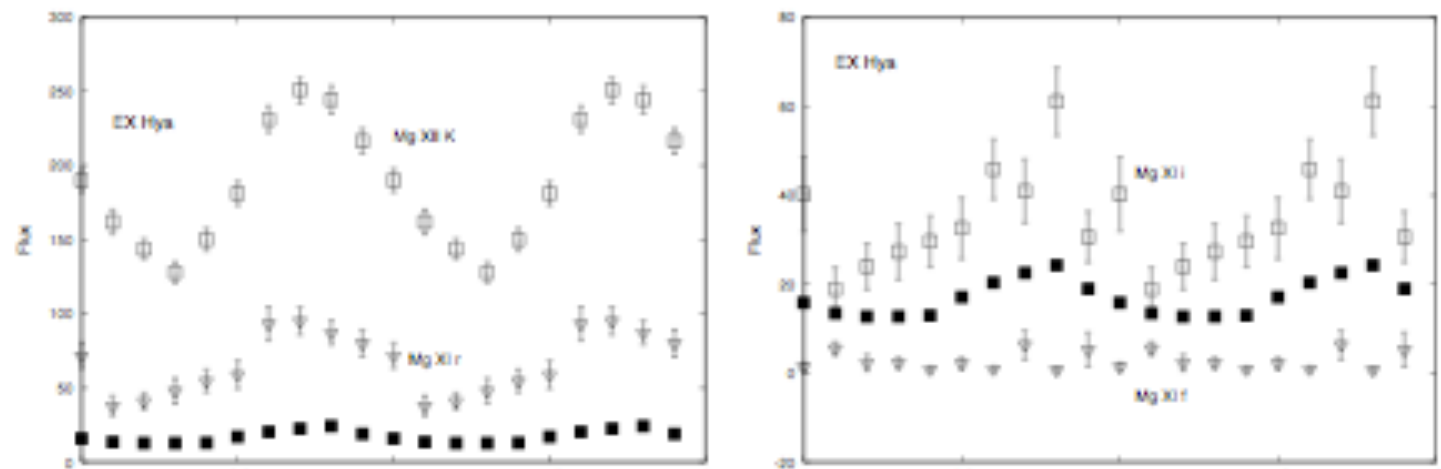


Fig. 38.— Light curve for EX Hya folded at the spin phase: (left) Mg XII  $K\alpha$  and Mg XI r; (right) Mg XI i and f. Filled squares = neighboring continuum.



# EX Hydrae: Spin Phase folding Ne and Mg lines

Fig. 39.— Light curve for EX Hya folded at the spin phase: (left) Ne X  $K\alpha$  and Ne IX r; (right) Ne IX i and f. Filled squares = neighboring continuum.

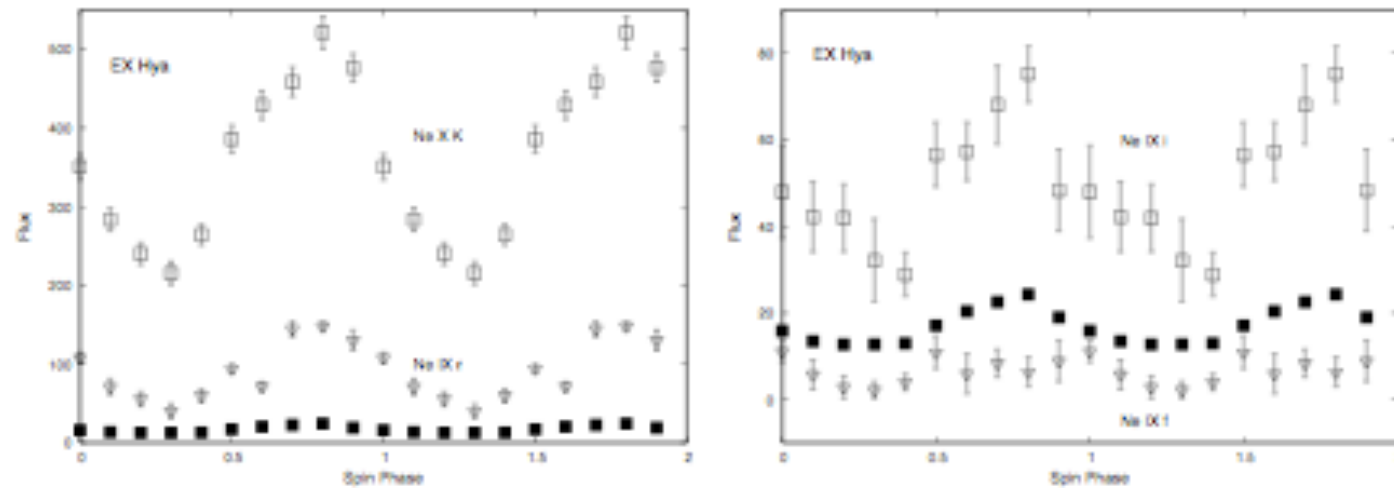
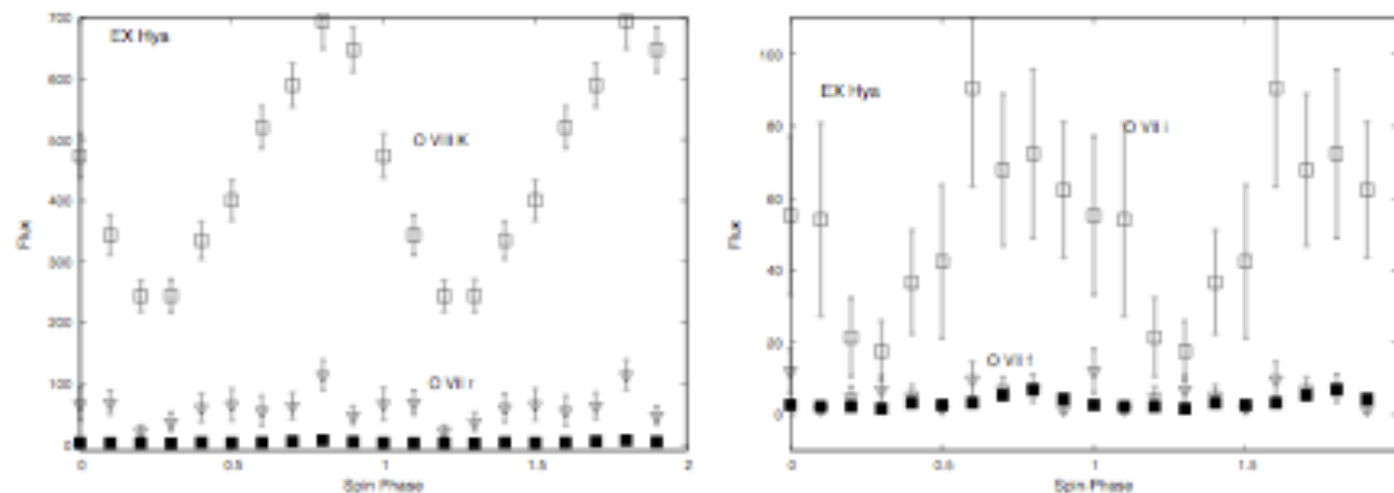


Fig. 40.— Light curve for EX Hya folded at the spin phase: (left) O VIII  $K\alpha$  and O VII r; (right) O VII i and f. Filled squares = neighboring continuum.



# EX Hydrae : Spin phase modulation

The  $K\alpha$  line exhibits a larger fractional variation than do any of the triplet lines at the lower ionization energies (e.g., Ne, O) than at the high ionization energies (e.g., Fe, S).

A comparison of the Fe and O lines shows:

- Fe XXVI  $K\alpha$  line essentially tracks the Fe XXV r line in amplitude and phase.
- In contrast, the O VIII  $K\alpha$  line varies by ~75% while the O VII triplet r line is relatively constant within the errors, varying by perhaps ~20%.
- Work in progress

# Conclusions

- Collisionally ionized plasmas appear to dominate the X-ray spectra of several CVs (magnetic as well as non-magnetic)
- High densities are required in most CVs
- Significant broadening of Fe XXV is seen U Gem in outburst indicating high velocity gas.
- Broadening is also seen in Fluorescent Fe in U Gem but during the quiescence state
- Broad Fe XXV line with a flat-top profile is seen in SS Cyg in outbursts: high velocity winds or outflows are indicated
- Fluorescent Fe line is red-shifted by  $\sim 2300 \pm 500$  km/s in SS Cyg

# Conclusions

- Ne/O Abundance: ONe models of WDs preferred over CO models
- AM Her: Phase resolved spectroscopy shows that the line centers of Mg XII, Si XVI, resonance line of Fe XXV, and Fe XXVI emission modulated by 1000 km/s indicating bulk motion of ionised material in the accretion column
- EX Hya: phase resolved spectroscopy shows modulation of line intensities from O to Fe with varying degrees for different ionization stages
- Need large areas with very high resolution

# Collaborators

- V. R. Rana (former TIFR student, now at Caltech, NuStar Group)
- V. Girish (TIFR Post-doc, now at ISAC, Bangalore)
- E. M. Schlegel and H. V. Shipley (U of Texas-San Antonio)
- P. E. Barrett (US Naval Observatory)

Thanks

# Global Fit Approach

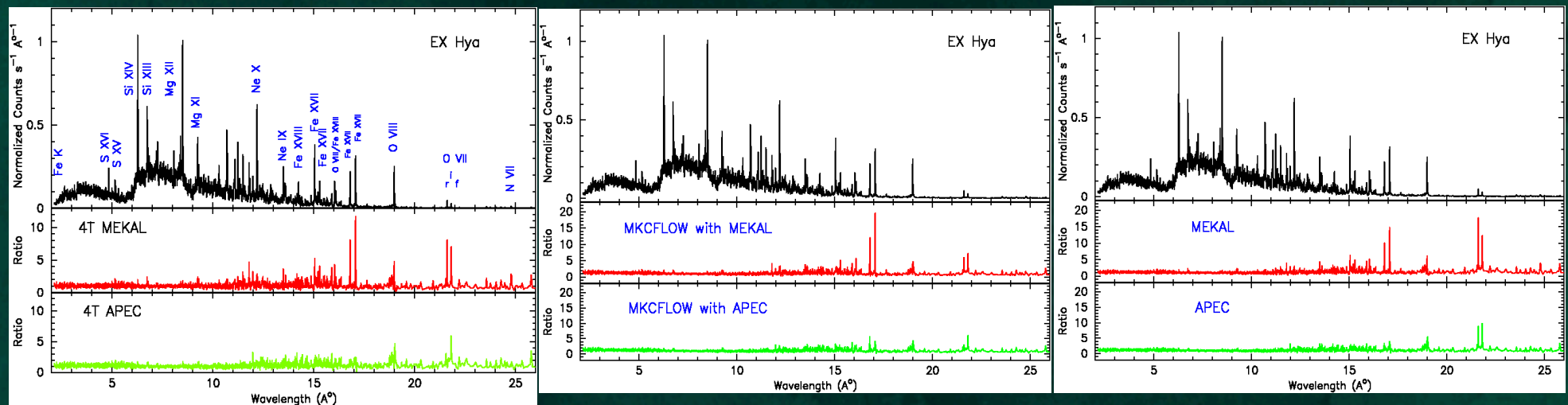
EX Hya: Brightest IP observed with Chandra HETG

APEC & MEKAL: Two competing plasma codes

Discrete temperature  
(4T)

Cooling flow model

Stratified accretion  
column multi-temp



- APEC model provides better fit to emission lines in overall MEG wave band. In particular 5-15 Å wave length range and Fe XVII lines around 17 Å.
- Improvement in the fit is independent of the spectral models used.
- This is most likely due to deficiencies in the MEKAL with respect to APEC plasma code.

